Temperature dependence piezoreflectance study of the effect of doping MoS_2 with rhenium

2000 J. Phys.: Condens. Matter 12 3441

(http://iopscience.iop.org/0953-8984/12/14/319)

J. Phys.: Condens. Matter **12** (2000) 3441–3449. Printed in the UK PII: S0953-8984(00)09690-9

Temperature dependence piezoreflectance study of the effect of doping MoS_2 with rhenium

K K Tiong†§, T S Shou† and C H Ho‡

† Department of Electrical Engineering, National Taiwan Ocean University, Keelung 202, Taiwan, Republic of China

‡ Department of Electronic Engineering, Kuang Wu Institute of Technology and Commerce, Peitou, Taipei 112, Taiwan, Republic of China

E-mail: kktiong@ind.ntou.edu.tw

Received 18 November 1999

Abstract. We have recorded piezoreflectance (PzR) spectra at 15 K over the energy range 1.5–2.5 eV for undoped, 0.5% and 1% rhenium- doped (Re-doped) MoS_2 single crystals to examine the effect of dopant on the spectral features near the direct band- edge excitonic transitions. More elaborate temperature dependences of the excitonic features A and B of the Re-doped MoS_2 single crystals in the range 15 to 300 K have also been obtained using PzR. The energies and broadening parameters of the A and B excitons of the Re-doped MoS_2 samples have been determined accurately via a detailed line shape fit of the PzR spectra. The parameters that describe the temperature variation of the energies and broadening functions of the excitonic transitions are analysed. A plausible suggestion will be put forth to explain the role of rhenium in affecting the variation of the excitonic transitions.

1. Introduction

Molybdenum disulphide is an important member of the layered type transition metal dichalcogenide family [1], MX_2 where M = Mo or W and X = S or Se. The material is of interest as a potential candidate in a variety of important technologies such as solid lubricants [2–4], photovoltaic solar cells [5–8], hydrosulphurization catalysts [9] etc. Recent efforts in improving the photoconductivity of layered type transition metal dichalcogenides have been implemented by doping the samples with either rhenium or niobium [10]. Most of the studies were on diselenides [10–12], due probably to the better performance of the material in solar cell application. However for practical application of the material, the resource abundance of naturally occurring molybdenite [14] and non-toxicity of sulphur should offer a definite advantage for disulphides over diselenides even though the diselenides have been shown to be more efficient in the solar cell conversion process. Moreover, it has been found that the doping of MoS_2 with rhenium [13] showed quite a marked difference from that of $MoSe_2$ [12]. Rhenium-doped $MoSe_2$ retains the crystal structure of 2H-$MoSe_2$ with a slight widening of the van der Waals gap [12]. The dopant plays the role of donor impurity with enhancement of electrical conductivity and photocurrent gain [10]. A reduction of electrical anisotropy along and perpendicular to the *c*-axis is also observed [11, 12]. For Re-doped MoS_2, the rhenium dopant seems to serve more than just as an impurity donor. It is most

§ Author to whom correspondence should be addressed.

0953-8984/00/143441+09$30.00

likely that the rhenium transition ions can either substitute for the Mo metal ions interstitially or intercalate between the van der Waals gap resulting in a distortion of crystal structure [10, 13, 15]. The sandwich Re ions create stronger bonds than the original van der Waals forces and transform the two-layer hexagonal MoS_2 (2H-MoS_2) into three-layer rhombohedral MoS_2 (3R-MoS_2). The observation of the change in crystal structure of Re-doped MoS_2 was confirmed previously [13, 15]. In addition, enhancement of electrical conductivity and a reduction of electrical anisotropy along and perpendicular to the crystal c-axis were also observed [13]. The transformation of 2H-MoS_2 into 3R-MoS_2 by doping with rhenium is perhaps not too surprising as it has been found that naturally occurring 3R-MoS_2 is consistently rich in certain minor elements such as Re, Nb etc [14]. Despite the potentially attractive fundamental research offered by Re-doped MoS_2, very few studies concerning the influence of rhenium dopant on the electrical and optical properties of the material have been attempted [13, 16].

In this paper, we have recorded the PzR [17, 18] spectra for undoped, 0.5% and 1% Re-doped MoS_2 over the energy range 1.5–2.5 eV at 15 K. An elaborate temperature dependence of the spectral features near the direct band-edge excitonic transitions of the Re-doped MoS_2 in the range 15 to 300 K has also been obtained using PzR. From a detailed line shape fit with a form of the Aspnes equation of the derivative Lorentzian line shape [17, 19], the energies of the band edge excitonic transitions are determined accurately. The temperature variations of the transition energies of A and B excitons are analysed by the Varshni equation [20] and an expression containing the Bose–Einstein occupation factor for the phonons [21, 22]. The temperature dependence of the broadening function has also been studied in terms of a Bose–Einstein equation that contains the electron (exciton)–longitudinal optical (LO) phonon coupling constant [21, 22]. The physical role of rhenium in influencing the electronic states of the MoS_2 crystal will also be discussed.

2. Experiment

Rhenium-doped MoS_2 single crystals have been grown by the chemical vapour transport method with Br_2 as a transport agent. The total charge used in each growth experiment was about 10 g. The stoichiometrically determined weight of the doping material was added in the hope that it would be transported at a rate similar to that of Mo. The quartz ampoule containing Br_2 ($\sim$5 mg cm^{-3}) and uniformly mixed elements (99.99% pure Mo, Re and S) was sealed at 10^{-6} Torr. The ampoule was then placed in a three-zone furnace and the charge prereacted for 24 h at 800 °C with the growth zone at 950 °C, preventing the transport of the product. The temperature of the furnace was increased slowly to avoid any possibility of explosion due to the exothermic reaction between the elements. The furnace was then equilibrated to give a constant temperature across the reaction tube, and programmed over 24 h to produce the temperature gradient at which single-crystal growth took place. Optimal results were obtained with a temperature gradient of approximately 960 $\rightarrow$ 930 °C. Single crystalline platelets up to 10 $\times$ 10 mm^2 surface area and 2 mm in thickness were obtained. MoS_2 crystallizes with 2H or 3R structure while ReS_2 crystallizes in a distorted C6 structure [1], so that we do not expect the two solid solutions to be miscible. It was found that a 5% nominal doping of MoS_2 prevented the growth of single crystals [13].

The rhenium composition was estimated by energy dispersive x-ray analysis (EDX). A considerable discrepancy exists between the nominal doping ratios and those determined by EDX. The nominal concentration x is much larger than the actual one. Because no Re could be detected in EDX even though this method is sensitive for concentrations $\geqslant$1%, we conclude that Mo and Re metals are most likely chemically transported at different rates and most of

the doping material must remain in the 'untransported' residual charge. For the experiments, the concentration of rhenium is taken to be the nominal starting composition.

The PzR measurements were performed on a standard experimental set-up described elsewhere. The low temperature measurements were achieved via an RMC model 22 closed-cycle cryogenic refrigerator equipped with a model 4075 digital thermometer controller. For high temperature experiments the PZT was mounted on one side of a copper finger of an electrical heater, which enables us to stabilize the sample temperature. The measurements were made between 15 and 300 K with a temperature stability of 0.5 K or better.

3. Results and discussion

Displayed in figure 1 are the PzR spectra over the range 1.5– 2.5 eV at 15 K for 0.5% Re-doped (top), 1% Re-doped (middle) and undoped (bottom) MoS_2 single crystals. The spectra are characterized by two prominent excitonic transitions, A and B excitons. In the case of undoped MoS_2, a higher series of A exciton, denoted as A_2, is also detected. In order to determine the positions of the transitions accurately, we performed a theoretical line shape fitting. The functional form used in the fitting procedure corresponds to a first derivative Lorentzian line shape function of the form [17, 19]

$$\frac{\Delta R}{R} = \mathrm{Re} \sum_{j=1} A_j \, \mathrm{e}^{\mathrm{i}\Phi_j} (E - E_j + \mathrm{i}\Gamma_j)^{-n_j} \tag{1}$$

where the subscript j refers to the type of interband transition, A_j and Φ_j are the amplitude and phase of the line shape, E_j and Γ_j are the energy and broadening parameter of the transition and the value of n_j depends on the origin of the transition. For the first derivative functional form, $n = 2.0$ is appropriate for the bounded states, such as excitons or impurity transitions, while $n = 0.5$ is applicable for three-dimensional critical point interband transitions [19]. The least-squares fits using equation (1) with $n = 2$ can be achieved and the fits are shown as solid curves in figure 1. The fits yield the parameters A_j, E_j and Γ_j. The obtained values of E_j are indicated as arrows and denoted as A_1, A_2 and B. The nomenclature used here follows closely that of Wilson and Yoffe [1] and Beal *et al* [23]. The values of E_j obtained here show a general agreement with slight deviation from the corresponding low temperature transmission data of Beal *et al* [23]. We believed the derivative nature of the PzR spectra should offer better accuracy. The fitted values of E_j are displayed in table 1 together with the relevant works of [23] for comparison. In this study, we have found no discernible difference between the fitted values of E_j for the 0.5% and 1% Re-doped samples. This is most probably a consequence of immiscibility of MoS_2 and ReS_2 crystals [11–13]. Most of the rhenium must remain in the 'untransported' stage and the actual compositions of rhenium in the doped samples must be smaller than the nominal starting material. It is likely that a similar amount of rhenium dopant is absorbed into the doped sample for both nominal starting compositions. Hence, these samples will be referred to as undoped and Re-doped MoS_2 when no ambiguity is raised. The prominent A and B excitons are observed to be red-shifted. The energy positions of A and B excitons are measured accurately with the PzR experiment. The splittings of excitons A and B ($\Delta_{BA} = E_B - E_A$) are determined to be 151 ± 3 meV for Re-doped MoS_2 and 208 ± 6 meV for undoped MoS_2. These numbers agreed well with the corresponding transmission data of Beal *et al* [23] and the wavelength modulated reflectance (WMR) spectra of Fortin and Raga [25]. In the case of the WMR data of Fortin and Raga, their observed signature, B^* is almost certain to be due to the presence of 3R-MoS_2 in their 2H-MoS_2 sample. For undoped MoS_2, the excitons A and B Rydberg series can be described by the three-dimensional Mott–Wannier excitons [23, 26, 27] which follow closely the relations,

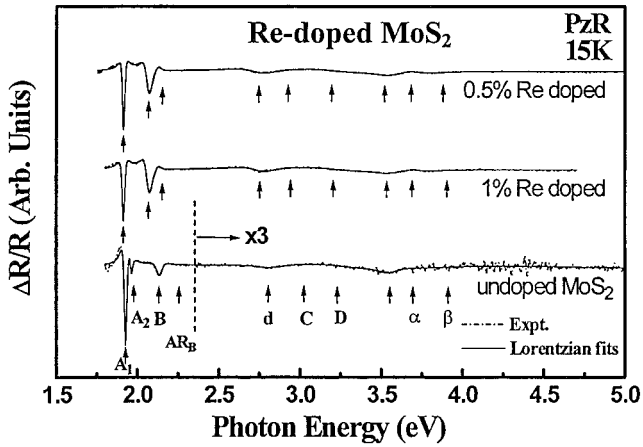

Figure 1. Piezoreflectance spectra of undoped, 0.5% and 1% Re-doped MoS_2 at 15 K over energy range 1.5 to 2.5 eV.

$E_A = 1.971 - 0.042/n^2$ and $E_B = 2.267 - 0.134/n^2$ [28], where $n = 1$, 2, 3 and 4. The broader linewidth of the B exciton probably prevents the detection of higher Rydberg series. For Re-doped MoS_2, only $n = 1$ Rydberg series for both excitonic transitions are observed. It has been shown that excitons for the three-layer rhombohedral MoS_2 are more appropriately described by the two-dimensional Mott–Wannier excitons [23, 26, 27]. The non-detection of higher series is an inherent nature of the two-dimensional Wannier excitons [26]. The physical origin of the measured difference in the energy splitting of A and B excitons Δ_{BA} for the Re-doped and undoped MoS_2 may be understood as follows. From the more recent theoretical and experimental studies [28–30], the A and B excitons are attributed to the smallest direct transitions at the $\boldsymbol{K}$ point of the Brillouin zone split by interlayer interaction and spin–orbit splitting [28, 29]. The A exciton belongs to $\boldsymbol{K}_4$ to $\boldsymbol{K}_5$ while the B exciton corresponds to $\boldsymbol{K}_1$ to $\boldsymbol{K}_5$ optical transitions. The $\boldsymbol{K}$ states have been shown by Coehoorn *et al* [28, 29] to be predominantly metal d states with a small contribution from the non-metal p states. During growth of Re-doped MoS_2, the rhenium transition ions can either substitute for the Mo metal or intercalate between the two layers that are bonded by the van der Waals forces. The immiscibility of ReS_2 and MoS_2 [25] means that only a small quantity of Re can be absorbed into the doped MoS_2 and this tiny amount would probably perturb the Mo content in the $\boldsymbol{K}$ states slightly. The resulting splitting should open up slightly if no other mechanisms are involved. This plausible deduction is inferred from other experimental works on mixed crystals of MoS_2 with either WS_2, WSe_2 or $MoSe_2$ where larger anion or cation masses will result in a widening of Δ_{BA}. However, the measured shrinkage of Δ_{BA} shows the opposite trend. Other mechanisms such as the well known process of intercalation which usually involves a distortion of crystal structure and a variation of the electronic states of the synthesized compounds [31] may be responsible. It is very likely that the Re ions either substitute for the Mo metal ions interstitially or intercalate between the van der Waals gaps and stabilize the 3R polytype of MoS_2. The resulting van der Waals forces of 3R-MoS_2 should be weaker than the 2H polytype and this is reflected by the measured reduction in Δ_{BA}.

In figure 2, PzR spectra showing the prominent exciton A and B features for 0.5% Re-doped MoS_2 at several representative temperatures are displayed. The PzR spectra for 1% Re-doped MoS_2 are similar and will not be shown here. The energies and linewidths of A and B excitons

Table 1. Energies of the excitons A and B for the undoped, 0.5% and 1% Re-doped MoS_2 crystals for reflected signals off the van der Waals surface.

	A (eV)	B (eV)
Undoped MoS_2[a]	1.928	2.136
0.5% (1%) Re-doped MoS_2[a]	1.915	2.066
2H-MoS_2[b]	1.910	2.112
3R-MoS_2[b]	1.908	2.057

[a] This work using PzR at 15 K.
[b] Transmission data at 5 K from [23].

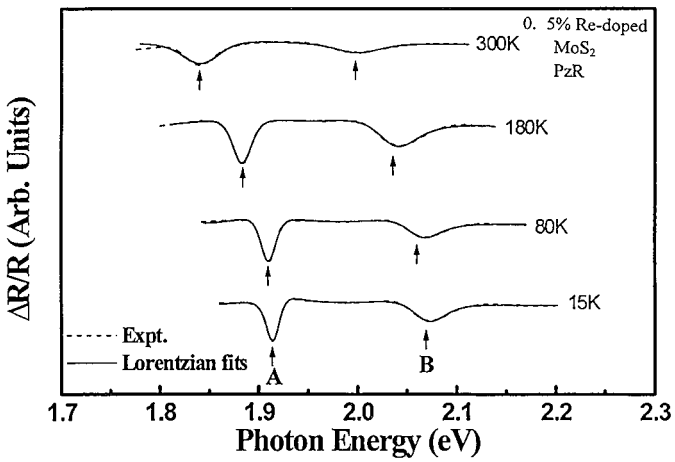

Figure 2. Piezoreflectance spectra of the A and B excitonic transitions for 0.5% Re-doped MoS_2 at 15, 80, 180 and 300 K showing their temperature dependence. (1% Re-doped MoS_2 shows similar dependence.)

are determined accurately using equation (1). The energies of both excitonic transitions show the general trend of up-shifting as the temperature is lowered. The linewidths also become narrower in the process. The temperature variations of the energies of A and B excitons for the doped MoS_2 are displayed in figure 3. The dashed curves in figure 3 are the least-squares fits to the Varshni empirical relationship [20]

$$E_i(T) = E_i(0) - \frac{\alpha_i T^2}{(\beta_i + T)} \tag{2}$$

where i = A or B, $E_i(0)$ is the excitonic transition energy at 0 K and α_i and β_i are constants referred to as the Varshni coefficients. The constant α_i is related to the electron (exciton)–phonon interaction and β_i is closely related to the Debye temperature. For the doped MoS_2, the fitted values for exciton A are $E(0) = 1.918 \pm 0.005$ eV, $\alpha = 0.41 \pm 0.05$ meV K^{-1} and $\beta = 175 \pm 50$ K, and for exciton B $E(0) = 2.072 \pm 0.005$ eV, $\alpha = 0.43 \pm 0.05$ meV K^{-1} and $\beta = 180 \pm 50$ K. These numbers are quite similar to other layered structure transition metal dichalcogenide compounds [24]. The temperature dependence of the excitonic transition energies $E_A(T)$ and $E_B(T)$ of the doped and undoped MoS_2 can also be fitted (solid curves)

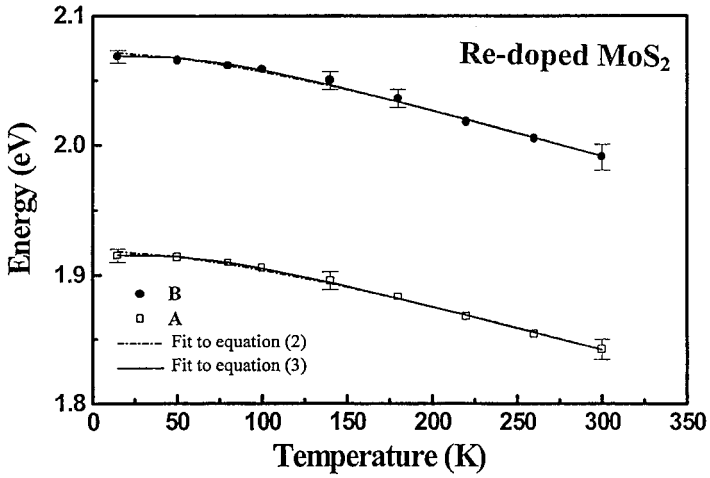

Figure 3. Temperature variation of the energies of the A and B excitons of the Re-doped MoS_2. Dashed lines are least-squares fits to equation (2) and solid lines to equation (3).

by the expression

$$E_i(T) = E_{iB} - a_{iB}\left\{1 + \frac{2}{[\exp(\Theta_{iB}/T) - 1]}\right\} \tag{3}$$

where $i = A$ or B, a_{iB} represents the strength of the electron (exciton)–phonon interaction and Θ_{iB} corresponds to the average phonon temperature. For the doped samples, the fitted values for exciton A are $E_{AB} = 1.954 \pm 0.01$ eV, $a_{AB} = 39 \pm 12$ meV and $\Theta_{AB} = 215 \pm 50$ K, and for exciton B $E_{BB} = 2.108 \pm 0.01$ eV, $a_{BB} = 40 \pm 12$ meV and $\Theta_{BB} = 210 \pm 50$ K. Again, these values are typical of all layered structure transition metal dichalcogenides [24].

The experimental values of $\Gamma_i(T)$ (half width at half maximum (HWHM)) of A and B excitons at several temperatures between 15 and 300 K as obtained from the line shape fit with equation (1) for 0.5% and 1% Re-doped MoS_2 are displayed in figure 4. Linewidth broadening nearly independent of temperature below 100 K characterizes both excitonic transitions. The temperature independent broadening characteristics of the excitonic transitions for the layered structure transition metal dichalcogenides at temperature below 100 K has been observed previously [24, 25]. The rather high value of this temperature is attributed to the high value of the exciton reduced mass for the MoS_2 crystal (see [25] and references therein). The temperature dependence of the broadening parameters of semiconductors can be analysed by the expression [21, 22]

$$\Gamma_i(T) = \Gamma_{i0} + \frac{\Gamma_{iLO}}{[\exp(\Theta_{iLO}/T) - 1]} \tag{4}$$

where $i = A$ or B. Γ_{i0} represents the broadening resulting from temperature independent mechanisms, such as electron–electron interaction, impurity, dislocation and alloy scattering and the second term originates from the electron (exciton)–LO phonon (Fröhlich) interaction. The quantity Γ_{iLO} represents the strength of the electron (exciton)–LO phonon coupling while Θ_{iLO} is the LO phonon temperature. The solid curves in figure 4 are the least- squares fits to equation (4). The parameters Γ_{i0}, Γ_{iLO} and Θ_{iLO} are evaluated for A and B excitons. These quantities together with that of the undoped MoS_2 and the ternary system $Mo_{1-x}W_xS_2$ from previous work [24] are listed in table 2 for comparison.

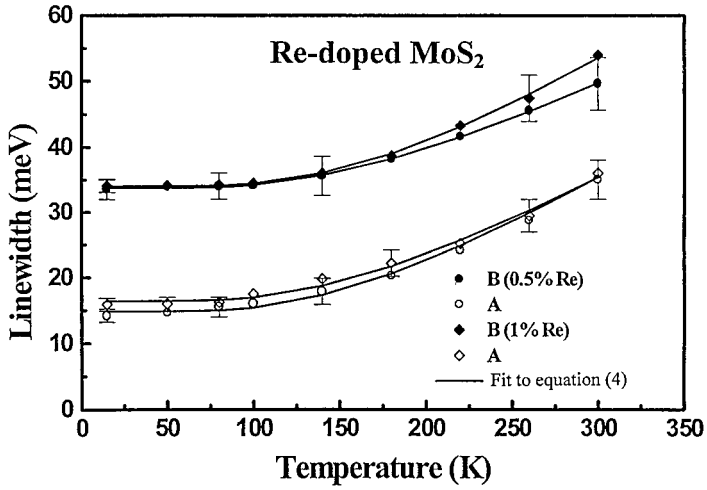

Figure 4. Temperature variation of the linewidths of the A and B excitons for 0.5% and 1% Re-doped MoS_2. Solid lines are least-squares fits to equation (4).

Table 2. Values of the parameters which describe the temperature dependence of the of the broadening function of undoped, 0.5% and 1% Re-doped MoS_2 using equation (4). Relevant values for $Mo_{1-x}W_xS_2$ are included for comparison.

Feature	Materials	Γ_0 (meV)	Γ_{LO} (meV)	Θ_{LO} (K)
A_1	0.5% Re-doped MoS_2[a]	15.0 ± 1.0	92 ± 20	510 ± 50
	1% Re-doped MoS_2[a]	16.4 ± 1.0	85 ± 16	510 ± 50
	Undoped MoS_2[b]	18.0 ± 1.0	75 ± 20	560 ± 50
	$Mo_{0.7}W_{0.3}S_2$[b]	30.0 ± 1.0	65 ± 20	560 ± 50
	$Mo_{0.5}W_{0.5}S_2$[b]	40.5 ± 1.0	85 ± 20	540 ± 50
	$Mo_{0.3}W_{0.7}S_2$[b]	41.6 ± 1.0	60 ± 20	530 ± 50
	WS_2[b]	20.0 ± 12	50 ± 20	520 ± 50
B	0.5% Re-doped MoS_2[a]	33.6 ± 1.0	72 ± 20	510 ± 50
	1% Re-doped MoS_2[a]	34.0 ± 1.0	90 ± 17	520 ± 50
	Undoped MoS_2[b]	37.4 ± 2.0	75 ± 35	560 ± 50
	$Mo_{0.7}W_{0.3}S_2$[b]	62.8 ± 2.0	85 ± 25	560 ± 50
	$Mo_{0.5}W_{0.5}S_2$[b]	61.9 ± 2.0	85 ± 30	540 ± 50
	$Mo_{0.3}W_{0.7}S_2$[b]	62.2 ± 2.0	75 ± 25	530 ± 50
	WS_2[b]	37.5 ± 2.0	90 ± 40	520 ± 50

[a] This work.
[b] [24].

From both fitting procedures using equations (2) and (3), the parameters obtained are consistent. For example, at the high temperature limit, the value of α_i of equation (2) is related to a_{iB} and Θ_{iB} of equation (3) by the relation $\alpha_i \sim 2a_{iB}/\Theta_{iB}$. Within the error limit, this relation holds fairly well. The temperature shifts of the energies of the excitonic transitions are due to both the lattice constant variations and interactions with relevant acoustic and optical phonons. From the theoretical consideration of the interaction, the resulting Θ_{iB} will be

significantly smaller than the values of Θ_{iLO}. Our results agreed favourably with the theory [21].

From table 2, the values of Γ_{i0} for 0.5% and 1% Re- doped MoS_2 for both A and B excitons are slightly smaller than that of the undoped sample. This means that the Re dopant probably introduces, if any, very small impurity or alloy scattering into the system. As has been said earlier the Re ions are most likely intercalated between the van der Waals gap and stabilize the rhombohedral 3R phase of the MoS_2 crystal instead of forming the ternary $Mo_{1-x}Re_xS_2$ system. Our experimental observations thus far support this assertion. We also note that sharper line shapes of A and B excitons have been consistently observed for 3R-MoS_2 crystals [23]. A comparison of the fitted values of Γ_{i0} for 0.5% and 1% Re-doped MoS_2 seem to indicate a slightly higher value for the latter sample. We suspect that for the 1% Re-doped sample it is quite possible that some of the dopant may remain in the 'untransported' stage, which shows up in the experiment as impurity scattering and results in a slightly broader HWHM. However, from the close similarity of the experimental line shapes and of the fitted parameters, the observed difference may not be significant enough to account for the effect of rhenium induced impurity scattering. The apparent ambiguous reasoning is not unreasonable considering the rather small quantity of dopant involved.

4. Summary

In summary we have measured the temperature dependence of the energies and broadening parameters of the direct band-edge excitonic transitions of 0.5% and 1% Re-doped MoS_2 using PzR in the temperature range 15 to 300 K. From the experimental observations and detailed analysis of the broadening parameters and energies of the excitonic features A and B, we can infer that the rhenium ions are most likely intercalated between the van der Waals gaps and stabilize the formation of 3R-MoS_2. As a result the electronic states of the MoS_2 crystals are modified with a reduction of the energy splitting of A and B excitons.

Acknowledgments

The authors wish to thank Professor Y S Huang of the Department of Electronic Engineering of National Taiwan University of Science and Technology for several helpful technical discussions. This work was supported by the National Science Council of the Republic of China under project No NSC89-2112-M-019-002.

References

[1] Wilson J A and Yoffe A D 1969 *Adv. Phys.* **18** 193
[2] Martin J M, Donnet C and Mogne J L 1993 *Phys. Rev.* B **48** 10 583
[3] Yanagisawa M 1993 *Wear* **168** 167
[4] Fleischauer P D 1987 *Thin Solid Films* **154** 309
[5] Tributsch H 1977 *Z. Naturf.* a **32** 972
[6] Kam K K and Parkinson B A 1982 *J. Phys. Chem.* **86** 463
[7] Li S J, Bernede J C, Pouzet J and Jamali M 1996 *J. Phys.: Condens. Matter* **8** 2291
[8] Jager-Waldau A, Lux-Steiner M, Jager-Waldau R, Burkhardt R and Bucher E 1990 *Thin Solid Films* **189** 339
[9] Grange P and Delmon B 1974 *J. Less-Common Met.* **36** 353
[10] Legma J B, Vacquier G, Traorè H and Casalot A 1991 *Mater. Sci. Eng.* B **8** 167
[11] Levy F, Schmid P and Berger H 1976 *Phil. Mag.* **24** 1129
[12] Agarwal M K, Patel P D and Gupta S K 1993 *J. Cryst. Growth* **129** 559
[13] Tiong K K, Liao P C, Ho C H and Huang Y S 1999 *J. Cryst. Growth* **205** 543
[14] Clark A H 1970 *N. Jahrbuch Mineral. Monatshefte* **3** 33

[15] Zelikman A N, Indenbaum G V, Teslitskaya M V and Shalankova V P 1970 *Sov. Phys.–Crystallogr.* **14** 687
[16] Tiong K K and Shou T S 2000 *J. Phys.: Condens. Matter* submitted
[17] Pollak F H and Shen H 1993 *Mater. Sci. Eng.* R **10** 275
[18] Mathieu H, Allegre J and Gil B 1991 *Phys. Rev.* B **43** 2218
[19] Aspnes D E 1980 *Optical Properties of Semiconductors (Handbook on Semiconductors 2)* ed M Balkanski (Amsterdam: North-Holland) p 109
[20] Varshni Y P 1967 *Physica* **34** 149
[21] Lantenschlager P, Garriga M, Logothetidis S and Cardona M 1987 *Phys. Rev.* B **35** 9174
[22] Lantenschlager P, Garriga M, Vina L and Cardona M 1987 *Phys. Rev.* B **36** 4821
[23] Beal A R, Knights J C and Liang W Y 1972 *J. Phys. C: Solid State Phys.* **5** 3540
[24] Ho C H, Wu C S, Huang Y S, Liao P C and Tiong K K 1998 *J. Phys.: Condens. Matter* **10** 9317
[25] Fortin E and Raga F 1975 *Phys. Rev.* B **11** 905
[26] Beal A R and Liang W Y 1976 *J. Phys. C: Solid State Phys.* **9** 2459
[27] Chuang S L 1995 *Physics of Optoelectronic Devices (Wiley Series in Pure and Applied Optics)* ed J W Goodman (New York: Wiley)
[28] Coehoorn R, Haas C andde Groot R A 1987 *Phys. Rev.* B **35** 6203
[29] Coehoorn R, Haas C, Dijtkstra, Flipse C J F, de Groot R A and Wold A 1987 *Phys. Rev.* B **35** 6195
[30] Straub Th, Fauth K, Finteis Th, Hengsberger M, Claessen R, Steiner P, Hufner S and Blaha P 1996 *Phys. Rev.* B **53** 16 152
[31] Gandke T, Ley L and Cardona M 1977 *Phys. Rev. Lett.* **38** 872
Gandke T, Ley L and Cardona M 1977 *Phys. Rev. Lett.* **38** 1033